

# LCHO-CI method for the voltage control of exchange interaction in gated lateral quantum dot networks

Irene Puerto Gimenez,<sup>1,2</sup> Marek Korkusinski,<sup>1</sup> and Pawel Hawrylak<sup>1</sup>

<sup>1</sup>*Quantum Theory Group, Institute for Microstructural Sciences,  
National Research Council, Ottawa, Canada K1A 0R6*

<sup>2</sup>*Department of Fundamental Physics,  
University of La Laguna, Tenerife, Spain*

## Abstract

We present a computational LCHO-CI approach allowing for the simulation of exchange interactions in gated lateral quantum dot networks. The approach is based on single-particle states calculated using a linear combination of harmonic orbitals (LCHO) of each of the dots, and a configuration interaction (CI) approach to the interacting electron problem. The LCHO-CI method is applied to a network of three quantum dots with one electron spin per dot, and a Heisenberg spin Hamiltonian is derived. The manipulation of spin states of a three-spin molecule by applying bias to one of the dots is demonstrated and related to the bias dependence of effective exchange interaction parameters.

PACS numbers: 73.21.La, 73.23.Hk

## I. INTRODUCTION

The electron spin is a quantum two level system, a natural candidate for a qubit.<sup>1,2,3</sup> For this reason there is currently significant interest in coupling of individual electron spins localized at different spatial locations to realize quantum gates.<sup>2,3,4</sup> The coupling of the spins of localized interacting electrons is investigated using the Heisenberg Hamiltonian.<sup>4</sup> In this approach, the Coulomb interactions between electrons are reduced to the exchange coupling of their spins. The exchange interaction is parametrized by the exchange constants  $J$  dependent upon the specific implementation of the system.

In lateral gated quantum dot devices the spatial localization of individual electrons can be achieved by electrostatic coupling to their charge. To date, controlled confinement of one, two, and three spatially separated electrons has been demonstrated using the single,<sup>5,6</sup> double,<sup>7,8,9,10,11</sup> and triple<sup>12,13</sup> quantum dots, respectively. In these devices the electronic orbital degrees of freedom are manipulated directly by tuning the gate voltages, which, only through topology and statistics, translates into the control over the total spin of the system.<sup>14,15,16,17,18,19</sup> The voltage control of exchange coupling of two electrons in a single dot<sup>20</sup> and coherent control of spin states of a two-electron double-dot molecule<sup>10</sup> was recently demonstrated. The Heisenberg Hamiltonian appropriate for this two-spin system is parametrized by a single exchange constant  $J$ , whose magnitude defines the energy gap between the spin singlet and triplet eigenstates. By measuring this gap one can establish the dependence of  $J$  on the gate voltages. In a more complex network of  $N$  quantum dots with one spin per dot the number of exchange couplings needed is equal to the number  $N(N-1)/2$  of pairs. Even the simplest network of quantum dots, a triple quantum dot with one electron per dot, is described by a Heisenberg Hamiltonian with three exchange constants, depending nontrivially on the geometry of the system and the gate layout. This dependence was studied, e.g., by Scarola and Das Sarma,<sup>21</sup> who used the Hubbard, variational, and exact diagonalization approaches to demonstrate that the three-spin model is valid only for a limited range of triple-dot parameters. Mizel and Lidar<sup>14,15,16</sup> arrived at similar conclusions using the Heitler-London and Hund-Mülliken schemes to calculate the energy levels of three coupled dots with one electron per dot. In both cases the many-body effects were responsible for the appearance of higher-order terms in the effective spin Hamiltonian. The above studies were performed on triple-dot systems consisting of three dots on resonance, and did

not account for tuning of individual dots. In Ref. 13 we used the Hubbard model, and in Ref. 17 - the real-space wave functions coupled with the configuration-interaction technique (RSP-CI) to analyze the voltage-tunable three-electron gated lateral triple-dot device, however without mapping the resulting electronic properties onto the three-spin model. The Hubbard model is simple but requires parametrization of the Hamiltonian and cannot be directly linked to gates and applied voltages. The RSP-CI technique is very accurate but is difficult to implement for the future simulation of the time evolution of the quantum system.

The purpose of this work is to present a different computational approach, where linear combination of harmonic orbitals (LCHO) of each of the dots is used to describe tunneling of electrons, and the configuration interaction (CI) approach is used for the treatment of exchange and correlation in the interacting electron problem. The LCHO-CI method can then be directly used for the derivation of the effective Heisenberg Hamiltonian consistent with gate voltages, and for the simulation of the quantum operations.

We illustrate our method by analyzing the tunability of the exchange interaction and manipulation of the three spin system with voltage in a triangular quantum dot molecule. The triangular quantum dot molecule, realized recently by Gaudreau et al.,<sup>12</sup> is needed both for implementation of the quantum teleportation and creation of three-particle maximally entangled GHZ state.

## II. LCHO-CI METHOD FOR THE ELECTRONIC STRUCTURE OF QUANTUM DOT NETWORKS

### A. Single electron states in a quantum dot network

We describe here the LCHO method for the calculation of single electron states in a network of two-dimensional quantum dots. The method is illustrated on the example of a triple quantum dot.

We consider a triple quantum dot molecule created electrostatically by lateral gates<sup>12</sup> and approximate its lateral confinement potential by a sum of three two-dimensional Gaussians,  $V^{3QD} = -\sum_{i=1}^3 V_i \exp\left[-\frac{(x-x_i)^2+(y-y_i)^2}{d_i^2}\right]$ , with  $x_i$  and  $y_i$  being the coordinates of the center of  $i$ th Gaussian ( $i=1,2,3$ ),  $V_i$  being its depth, and  $d_i$  being its characteristic width. The depth and width of each Gaussian are functions of the gate voltages. The centers  $(x_i, y_i)$

of each dot are arbitrary but in the rest of the paper they are chosen to lie in the corners of an equilateral triangle. In the following we express all distances in effective Bohr radii  $a_B^* = \epsilon \hbar^2 / m^* e^2$  and all energies in units of effective Rydberg  $Ry^* = e^2 / 2\epsilon a_0^*$ , where  $e$  and  $m^*$  are the electron charge and effective mass, respectively, and  $\epsilon$  is the dielectric constant of the material. GaAs parameters  $m^* = 0.067 m_0$  and  $\epsilon = 12.4$  give  $Ry^* = 5.93$  meV and  $a_B^* = 97.9$  Å. Figure 1 shows the triple-dot confining potential for  $V_1 = V_2 = V_3 = 10 Ry^*$  and  $d_1 = d_2 = d_3 = 2.3 a_B^*$ . The dimensionless Hamiltonian for one electron in the potential of the triple quantum dot network is written in the following form:

$$H = -\frac{\partial^2}{\partial x^2} - \frac{\partial^2}{\partial y^2} - \sum_{i=1}^3 V_i \exp \left[ -\frac{(x - x_i)^2 + (y - y_i)^2}{d_i^2} \right]. \quad (1)$$

Since an exact analytical solution of the eigenvalue problem of the Hamiltonian (1) is not known, an approximate method is needed to calculate the energies and eigenvectors of one electron in the quantum dot network. Here we employ a quantum dot analog of the Linear Combination of Atomic Orbitals (LCAO) method. Expanding the Gaussian potential of dot  $i$  to second order in  $\vec{r}$ ,  $-V_i \exp \left[ -\frac{(\vec{r} - \vec{r}_i)^2}{d_i^2} \right] \approx -V_i + V_i \frac{(\vec{r} - \vec{r}_i)^2}{d_i^2}$ , results in the harmonic oscillator (HO) potential  $-V_i + \frac{1}{4} \Omega_i^2 (\vec{r} - \vec{r}_i)^2$ , with  $\Omega_i = 2\sqrt{V_i}/d_i$ . The eigenfunctions of this HO potential,  $\phi_{nm}^i(x, y) = \varphi_n^i(x - x_i) \varphi_m^i(y - y_i)$ , are products of the 1D HO eigenfunctions  $\varphi_n(t) = \left( \frac{1}{\pi l^2} \right)^{\frac{1}{4}} \left( \frac{l^{2n}}{2^n n!} \right)^{\frac{1}{2}} \left( \frac{t}{l^2} - \frac{d}{dt} \right)^n \exp \left( -\frac{t^2}{2l^2} \right)$ , where  $l = l_i = \sqrt{\frac{2}{\Omega_i}} = \left( \frac{d_i^2}{V_i} \right)^{\frac{1}{4}}$ . The first three states have the explicit form  $\varphi_0(t) = \left( \frac{1}{\pi l^2} \right)^{\frac{1}{4}} \exp \left( -\frac{t^2}{2l^2} \right)$ ,  $\varphi_1(t) = \sqrt{2} \left( \frac{1}{\pi l^2} \right)^{\frac{1}{4}} \left( \frac{t}{l} \right) \exp \left( -\frac{t^2}{2l^2} \right)$ ,  $\varphi_2(t) = \frac{1}{2\sqrt{2}} \left( \frac{1}{\pi l^2} \right)^{\frac{1}{4}} \left( -2 + \frac{4t^2}{l^2} \right) \exp \left( -\frac{t^2}{2l^2} \right)$ .

Hence, the molecular eigenfunctions of Eq. (1),  $|\xi_n\rangle$ , are written as linear combinations of the HO orbitals (LCHO) centered on each dot:

$$|\xi_n\rangle = \sum_{i=1}^{3n_o} a_i^n |\phi_i\rangle, \quad (2)$$

where  $a_i^n$  are the expansion coefficients and  $n_o$  is the number of HO orbitals per dot. To simplify notation, the three indices  $i$ ,  $n$ , and  $m$  of the HO eigenfunctions  $\phi_{nm}^i(x, y)$  have been replaced by the composite index  $i$ . Substituting this expression into the eigenvalue problem of Eq. (1) and multiplying on the left by  $\langle \phi_j |$  gives

$$\sum_{i=1}^{3n_o} \langle \phi_j | H | \phi_i \rangle a_i^n = \epsilon_n \sum_{i=1}^{3n_o} \langle \phi_j | \phi_i \rangle a_i^n.$$

Defining  $H_\phi$  as the Hamiltonian matrix in LCHO basis with elements  $\langle \phi_{00}^j | H | \phi_{00}^i \rangle = \int d\vec{r} \phi_{00}^{j*}(x, y) H \phi_{00}^i(x, y)$  and  $S_\phi$  as the overlap matrix with elements  $\langle \phi_{00}^j | \phi_{00}^i \rangle = \int d\vec{r} \phi_{00}^{j*}(x, y) \phi_{00}^i(x, y)$  allows us to write the generalized eigenvalue problem as

$$H_\phi \vec{a}^n = \epsilon_n S_\phi \vec{a}^n. \quad (3)$$

Now, defining a new vector

$$\vec{b}^n = (\sqrt{S_\phi}) \vec{a}^n \quad (4)$$

and multiplying Eq. (3) by  $(\sqrt{S_\phi})^{-1}$  on the left gives the standard eigenvalue problem

$$(\sqrt{S_\phi})^{-1} H_\phi (\sqrt{S_\phi})^{-1} \vec{b}^n = \epsilon_n \vec{b}^n. \quad (5)$$

In order to calculate  $(\sqrt{S_\phi})^{-1}$  the eigenvalue problem of the overlap matrix  $S_\phi V_S = V_S E_S$  is solved. Here  $V_S$  is the matrix with the eigenvectors and  $E_S$  is the diagonal matrix with the eigenvalues. Once the values of these two matrices are calculated,  $(\sqrt{S_\phi})^{-1}$  is obtained from  $(\sqrt{S_\phi})^{-1} = V_S E_S^{-1/2} V_S^T$ . Then the energies  $\epsilon_n$  (3) and eigenvectors (2) of the electron in the quantum dot network can be calculated using Eqs. (5) and (4). The accuracy of the solution depends on the number  $3n_o$  of HO orbitals included in the basis. Increasing the number of basis states increases the accuracy of results.

We now analyze the matrix elements of the Hamiltonian  $H_\phi$  in the basis  $\{|\phi_{00}^1\rangle, |\phi_{00}^2\rangle, |\phi_{00}^3\rangle\}$  showing explicitly the various contributions to the diagonal onsite energies and off-diagonal tunneling matrix elements:

$$H_\phi = \begin{bmatrix} \epsilon_1^d & t_{12} & t_{13} \\ t_{21} & \epsilon_2^d & t_{23} \\ t_{31} & t_{32} & \epsilon_3^d \end{bmatrix}. \quad (6)$$

If we label each of the three dots with indices  $i, j, k$ , we can express the diagonal matrix elements as

$$\begin{aligned} \epsilon_i^d &= \langle \phi_{00}^i | H | \phi_{00}^i \rangle \\ &= (-V_i + \Omega_i) + \langle \phi_{00}^i | \delta V^i | \phi_{00}^i \rangle + \langle \phi_{00}^i | V^j | \phi_{00}^i \rangle + \langle \phi_{00}^i | V^k | \phi_{00}^i \rangle, \end{aligned} \quad (7)$$

where we denote  $-V_i \exp \left[ -\frac{(x-x_i)^2 + (y-y_i)^2}{d_i^2} \right] = V_{HO}^i + \delta V^i$ , with  $V_{HO}^i$  being the 2D harmonic oscillator potential associated with dot  $i$ :  $V_{HO}^i = -V_i + \frac{1}{4}\Omega_i^2(\vec{r} - \vec{r}_i)^2$ . The first term in

(7),  $(-V_i + \Omega_i)$ , is the dominant term. It is the energy of the ground state of the harmonic oscillator potential  $V_{HO}^i$ . The second term,  $\langle \phi_{00}^i | \delta V^i | \phi_{00}^i \rangle$ , gives the correction due to non-harmonicity of the confining potential. The third and fourth terms,  $\langle \phi_{00}^i | V^j | \phi_{00}^i \rangle$  and  $\langle \phi_{00}^i | V^k | \phi_{00}^i \rangle$ , give the correction to the energy level of an isolated quantum dot  $i$  due to the presence of the other two quantum dot potentials.

The off-diagonal matrix elements describe electron tunneling from dot  $i$  to dot  $j$ . The tunneling matrix elements are determined by several contributions :

$$\begin{aligned} t_{ji} &= \langle \phi_{00}^j | H | \phi_{00}^i \rangle \\ &= (-V_i + \Omega_i) \langle \phi_{00}^j | \phi_{00}^i \rangle + \langle \phi_{00}^j | \delta V^i | \phi_{00}^i \rangle + \langle \phi_{00}^j | V^j | \phi_{00}^i \rangle + \langle \phi_{00}^j | V^k | \phi_{00}^i \rangle. \end{aligned} \quad (8)$$

The first term is directly proportional to the overlap between HO wave functions centered on different dots,  $\langle \phi_{00}^j | \phi_{00}^i \rangle$ , and is therefore small for dots which are far apart. The second term,  $\langle \phi_{00}^j | \delta V^i | \phi_{00}^i \rangle$ , is the correction due to non-harmonicity of the confining potential. The third term,  $\langle \phi_{00}^j | V^j | \phi_{00}^i \rangle$ , is a “two-centered” integral, as it involves a product of three functions centered at two different dots. The fourth term,  $\langle \phi_{00}^j | V^k | \phi_{00}^i \rangle$ , is a “three-centered” integral being thus the smallest term. This analysis of  $H_\phi$  matrix elements can also be applied to a larger HO basis including more shells ( $p, d, \dots$ ).

## B. Many-electron states in a quantum dot network

The many-electron Hamiltonian of the quantum dot network written in second quantization is

$$\hat{H} = \sum_j \epsilon_j c_j^\dagger c_j + \frac{1}{2} \sum_{ijkl} \langle ij | v | kl \rangle c_i^\dagger c_j^\dagger c_k c_l, \quad (9)$$

where  $c_m^\dagger$  and  $c_m$  are, respectively, the creation and annihilation operators of a particle on the spin-orbital itinerant (molecular) state  $m$ ,  $\psi_m(\vec{r}) = \xi_n(\vec{r}) \chi_{m_s}$ , where  $\chi_{m_s}$  is the electronic spinor corresponding to the spin  $m_s = \pm 1/2$ . Indices  $i, j, k$  and  $l$  run over spin-orbitals,  $\epsilon_j$  is the single-particle energy of an electron in the molecular state  $j$  and  $v$  is the dimensionless Coulomb potential,  $\frac{2}{|\vec{r}_2 - \vec{r}_1|}$ .

The Coulomb matrix elements (CMEs) in the itinerant basis are computed as linear combinations of CMEs in the localized HO basis

$$\langle ij | v | kl \rangle = \langle \chi_i | \chi_l \rangle \langle \chi_j | \chi_k \rangle \sum_{r=1}^{3n_o} \sum_{s=1}^{3n_o} \sum_{t=1}^{3n_o} \sum_{u=1}^{3n_o} a_r^i a_s^j a_t^k a_u^l \langle rs | v | tu \rangle, \quad (10)$$

where  $\langle rs|v|tu\rangle = \int d\vec{r}_1 \int d\vec{r}_2 \phi_r^*(\vec{r}_1) \phi_s^*(\vec{r}_2) \frac{2}{|\vec{r}_2 - \vec{r}_1|} \phi_t(\vec{r}_2) \phi_u(\vec{r}_1)$ . Using the identity  $\frac{2}{|\vec{r}_1 - \vec{r}_2|} = \frac{1}{\pi} \int \frac{d\vec{q}}{q} \exp[i\vec{q}(\vec{r}_1 - \vec{r}_2)]$ , we have

$$\langle rs|v|tu\rangle = \frac{1}{\pi} \int_0^\infty dq \int_0^{2\pi} d\vartheta F_{ru}^+(q, \vartheta) G_{ru}^+(q, \vartheta) F_{st}^-(q, \vartheta) G_{st}^-(q, \vartheta) \quad (11)$$

with  $F_{nm}^\pm(q, \vartheta) = \int_{-\infty}^\infty dt \varphi_n^*(t) \varphi_m(t) \exp[\pm itq \cos \vartheta]$  and  $G_{nm}^\pm(q, \vartheta) = \int_{-\infty}^\infty dt \varphi_n^*(t) \varphi_m(t) \exp[\pm itq \sin \vartheta]$ . These four integrals were obtained analytically and the double integral (11) over  $q$  and  $\vartheta$  was carried out numerically.

In order to obtain the energy levels and coherent eigenfunctions of  $N$  electrons in the quantum dot network we combine the LCHO method with the configuration interaction (CI) approach. In the CI method we build the  $N$ -electron basis out of all possible configurations of the  $N$  electrons on the molecular single-particle states. The many-electron eigenvalues and eigenfunctions are obtained by diagonalizing the Hamiltonian (9) in this  $N$ -electron basis of configurations. The number of these configurations  $n_C$  (and hence the dimension of  $H$ ) depends on the number of electrons  $N$  and the number  $n_{SO}$  of molecular spin-orbital states through  $n_C = \frac{n_{SO}!}{(n_{SO}-N)!N!}$ . In the case of as few as  $N = 3$  electrons, LCHO-CI calculations using only  $s$ -type HO orbital per dot gives 6 spin-orbitals, leading to  $n_C = 20$ . If for LCHO calculation we also include  $p$ -type HO orbitals, there are 18 molecular spin-orbitals, giving  $n_C = 816$ , while including also  $d$  HO orbitals gives  $n_C = 7140$ . The number of configurations in the 3-electron basis increases very rapidly with increasing number of HO orbitals in the one-electron calculations thus increasing the computational requirements.

One is primarily interested in quantum networks with one electron (one spin) per quantum dot. If one retains only one orbital per dot, the number of spin-orbitals is  $n_{SO} = 2N$ , and number of possible configurations is reduced to  $n_C = \frac{(2N)!}{N!N!}$ . For  $N = 10$  spins we already have 184756 configurations.

Further reduction in the number of configurations is possible. Since the Hamiltonian (9) is rotationally invariant, the Hamiltonian needs to be diagonalized only in one of the subspaces of lowest  $|S_z|$ . In what follows we present numerical results for the three-electron  $S_z = -1/2$  and  $S_z = -3/2$  states obtained with the LCHO-CI method.

### III. EFFECTIVE HEISENBERG MODEL

In order to establish a connection with quantum computation, it is convenient to approximate the Hamiltonian (9) of the system of singly-occupied dots in a quantum dot network by an effective Heisenberg spin Hamiltonian. For three electrons in three quantum dots this Hamiltonian takes the form

$$H^s = J_{12} \frac{1}{4} \vec{\sigma}_1 \vec{\sigma}_2 + J_{23} \frac{1}{4} \vec{\sigma}_2 \vec{\sigma}_3 + J_{13} \frac{1}{4} \vec{\sigma}_1 \vec{\sigma}_3, \quad (12)$$

where  $J_{ij}$  are the dimensionless exchange coupling constants, and  $\vec{\sigma}$  are the Pauli matrices. From this Hamiltonian the quantum gate  $\sqrt{SWAP}$  can be obtained by turning on one  $J_{ij}$  for an appropriate amount of time.<sup>3</sup> Combining this gate with single qubit gates we can obtain the *CNOT* gate, and *CNOT* together with one-qubit gates form the universal basis for quantum computing.<sup>1</sup>

Since  $H^s$  commutes with  $S_z$ ,  $H^s$  matrix is block diagonal in the basis of eigenvectors of  $S_z$ . Here we will treat the subspace  $S_z = -1/2$ . Taking the basis vectors  $\{|\downarrow\downarrow\uparrow\rangle, |\downarrow\uparrow\downarrow\rangle, |\uparrow\downarrow\downarrow\rangle\}$  we obtain

$$H^s = \frac{1}{4} \begin{bmatrix} J_{12} - J_{23} - J_{13} & 2J_{23} & 2J_{13} \\ 2J_{23} & -J_{12} - J_{23} + J_{13} & 2J_{12} \\ 2J_{13} & 2J_{12} & -J_{12} + J_{23} - J_{13} \end{bmatrix}. \quad (13)$$

Let us introduce a Jacobi basis of spin states:  $|\beta_a\rangle = \frac{1}{\sqrt{2}}(|\downarrow\downarrow\uparrow\rangle - |\downarrow\uparrow\downarrow\rangle)$ ,  $|\beta_b\rangle = \frac{1}{\sqrt{6}}(|\downarrow\downarrow\uparrow\rangle + |\downarrow\uparrow\downarrow\rangle - 2|\uparrow\downarrow\downarrow\rangle)$ , and  $|\beta_c\rangle = \frac{1}{\sqrt{3}}(|\downarrow\downarrow\uparrow\rangle + |\downarrow\uparrow\downarrow\rangle + |\uparrow\downarrow\downarrow\rangle)$ . The Heisenberg Hamiltonian (12) in the Jacobi basis has the following form:

$$H^s = \begin{bmatrix} -\frac{3}{4}J_{av} - \frac{3}{4}(J_{23} - J_{av}) & \frac{\sqrt{3}}{4}(J_{12} - J_{13}) & 0 \\ \frac{\sqrt{3}}{4}(J_{12} - J_{13}) & -\frac{3}{4}J_{av} + \frac{3}{4}(J_{23} - J_{av}) & 0 \\ 0 & 0 & \frac{3}{4}J_{av} \end{bmatrix}, \quad (14)$$

where  $J_{av} = (J_{12} + J_{23} + J_{13})/3$  is the average exchange constant. We see that if all exchange constants are equal the two states  $|\beta_a\rangle$  and  $|\beta_b\rangle$  are degenerate eigenstates with energy  $-\frac{3}{4}J_{av}$  and total spin  $S = 1/2$ , while the state  $|\beta_c\rangle$ , corresponding to total spin  $S = 3/2$ , has energy  $+\frac{3}{4}J_{av}$ . The Hamiltonian of the two degenerate states  $|\beta_a\rangle$  and  $|\beta_b\rangle$  is analogous to the Hamiltonian of a single spin in a magnetic field, where the magnetic field in the  $z$  direction is proportional to  $\frac{3}{4}(J_{23} - J_{av})$  and the magnetic field in the  $x$  direction is proportional to



$\frac{\sqrt{3}}{4}(J_{12} - J_{13})$ . This is why our system of three electrons in three dots can be thought of as a single coded qubit, whose logical states can be manipulated by varying the exchange constants.<sup>17</sup>

#### IV. RESULTS FOR A TRIPLE QUANTUM DOT NETWORK

We illustrate our theoretical approach on an example of a triple dot molecule with parameters given in Fig. 1. In section IV A we present the energies and eigenfunctions of one electron in the triple dot molecule calculated with LCHO method. In section IV B the energies of three electrons in the triple dot molecule obtained with LCHO-CI method are analyzed and compared with results obtained with Hubbard model.<sup>13</sup> In section IV C we analyze the triple dot molecule with one and three electrons when one of the dots is being biased. Finally, in section IV D we use the Heisenberg model to study the effects of biasing of one dot in a triple dot molecule with three electrons and compare the results with those obtained using LCHO-CI method.

##### A. One electron in a triple quantum dot

Figure 2 shows the set of one-electron energy levels in the triple quantum dot potential of Fig. 1 obtained by solving Eq. (3) for different LCHO basis sets:  $s : \{|\phi_{00}^1\rangle, |\phi_{00}^2\rangle, |\phi_{00}^3\rangle\}$ ,  $s+p : \{|\phi_{00}^1\rangle, |\phi_{10}^1\rangle, |\phi_{01}^1\rangle, |\phi_{00}^2\rangle, |\phi_{10}^2\rangle, |\phi_{01}^2\rangle, |\phi_{00}^3\rangle, |\phi_{10}^3\rangle, |\phi_{01}^3\rangle\}$ ,  $s+p+d$ , and  $s+p+d+f$ . The number of orbitals per shell in the spectra of a triple quantum dot is three times the number of orbitals per shell in the spectra of one quantum dot. Thus, we have three  $s$  orbitals, six  $p$  orbitals, nine  $d$  orbitals and so on.

The spectrum of one electron in the HO potential associated with one of the dots has electronic shells with level spacing  $\Omega_i = 2\sqrt{V_i}/d_i = 2.75 Ry^*$ . For the electron in an isolated Gaussian dot and assuming LCHO basis sets composed of  $sp$ ,  $spd$  and  $spdf$  HO shells one obtains  $s$ - $p$  level spacings of 2.44, 2.46 and 2.37  $Ry^*$  respectively. When the electron moves in the potential of the triple dot, the tunneling hybridizes shells from different dots and leads to molecular levels. Comparing the spectra of one electron in the triple-dot molecule for increasing number of HO shells in the LCHO basis we find that as the number of shells increases the low energy molecular levels decrease their energy and converge to a definite

value. The ground state of one electron in the symmetric triple-dot molecule is nondegenerate, and the first excited state is doubly degenerate. Figure 3 shows the eigenfunctions of these three levels ( $s$  orbitals  $\xi_1(\vec{r})$ ,  $\xi_2(\vec{r})$  and  $\xi_3(\vec{r})$ ) calculated using HO basis sets with different number of orbitals. Results obtained from calculations with only  $s$ -type HO orbitals in the LCHO basis are qualitatively the same as those obtained when more HO orbitals ( $p$ ,  $d$ ,  $f$ ) are included. Based on this conclusion, and anticipating a larger number of electrons in a quantum dot network, we will build the configurations for the three electron problem including one-electron energies and eigenfunctions obtained from calculations with the  $s$ -LCHO basis. Here we show typical numerical values for this  $s$ -LCHO calculation. The off-diagonal overlap matrix elements appearing in Eq. (3) are  $s = \langle \phi_{00}^j | \phi_{00}^i \rangle = 0.004088$ . The diagonal on-site energies defined in Eq. (7) are  $\epsilon^d = -8.647493 \text{ Ry}^*$  and have the contributions ( $i \neq j \neq k$ ):  $(-V_i + \Omega_i) = -7.250193 \text{ Ry}^*$ ,  $\langle \phi_{00}^i | \delta V^i | \phi_{00}^i \rangle = -0.166187 \text{ Ry}^*$ ,  $\langle \phi_{00}^i | V^j | \phi_{00}^i \rangle = -0.615556 \text{ Ry}^*$ , and  $\langle \phi_{00}^i | V^k | \phi_{00}^i \rangle = -0.615556 \text{ Ry}^*$ . On the other hand, the tunneling matrix elements hybridizing the atomic orbitals of adjacent dots, defined in Eq. (8), are  $t = -0.067162 \text{ Ry}^*$  and are composed of ( $i \neq j \neq k$ ):  $(-V_i + \Omega_i) \langle \phi_{00}^j | \phi_{00}^i \rangle = -0.029641 \text{ Ry}^*$ ,  $\langle \phi_{00}^j | \delta V^i | \phi_{00}^i \rangle = -0.014140 \text{ Ry}^*$ ,  $\langle \phi_{00}^j | V^j | \phi_{00}^i \rangle = -0.018489 \text{ Ry}^*$  and  $\langle \phi_{00}^j | V^k | \phi_{00}^i \rangle = -0.004892 \text{ Ry}^*$ . After solving Eq. (3), three energy levels corresponding to hybridized  $s$  shell and their eigenfunctions are obtained. The  $s$ -shell energy gap obtained between the ground state,  $|\xi_1\rangle$ , and the degenerate excited state,  $|\xi_2\rangle$  and  $|\xi_3\rangle$ , is  $\Delta\epsilon_S = 0.095 \text{ Ry}^*$ . We plot these energies in Fig. 2 (first spectrum on the left). The eigenfunctions of these three levels, plotted in the left-hand part of Fig. 3, are:

$$\begin{aligned}
|\xi_1\rangle &= 1/\sqrt{3(1+2s)}(|\phi_1\rangle + |\phi_2\rangle + |\phi_3\rangle), \\
|\xi_2\rangle &= 1/\sqrt{2(1-s)}(|\phi_1\rangle - |\phi_2\rangle), \\
|\xi_3\rangle &= 1/\sqrt{6(1-s)}(|\phi_1\rangle + |\phi_2\rangle - 2|\phi_3\rangle),
\end{aligned} \tag{15}$$

where  $s$  is the off-diagonal overlap matrix element. This number appears because the basis eigenfunctions are not orthogonal.

## B. Three electrons in a triple quantum dot network

Once the one-electron problem has been solved, we proceed to solve the three-electron Hamiltonian (9) using the configuration interaction method (CI). The first step is to build

the basis of three-electron configurations in which  $H$  is to be diagonalized. This is done for the subspaces  $S_z = -1/2$  and  $S_z = -3/2$ . There are nine three-electron configurations with  $S_z = -1/2$  obtained by distributing the three electrons among the six molecular spin-orbitals  $\{|\xi_i\rangle|\downarrow(\uparrow)\rangle, i = 1, 2, 3\}$  (for illustration see Fig. 4 (a)). These configurations can be grouped into six doubly-occupied configurations:  $|A\rangle = c_{1\downarrow}^+ c_{2\downarrow}^+ c_{1\uparrow}^+ |0\rangle$ ,  $|B\rangle = c_{1\downarrow}^+ c_{3\downarrow}^+ c_{1\uparrow}^+ |0\rangle$ ,  $|C\rangle = c_{1\downarrow}^+ c_{2\downarrow}^+ c_{2\uparrow}^+ |0\rangle$ ,  $|D\rangle = c_{2\downarrow}^+ c_{3\downarrow}^+ c_{2\uparrow}^+ |0\rangle$ ,  $|E\rangle = c_{1\downarrow}^+ c_{3\downarrow}^+ c_{3\uparrow}^+ |0\rangle$ , and  $|F\rangle = c_{2\downarrow}^+ c_{3\downarrow}^+ c_{3\uparrow}^+ |0\rangle$ , and three singly-occupied configurations:  $|G\rangle = c_{2\downarrow}^+ c_{3\downarrow}^+ c_{1\uparrow}^+ |0\rangle$ ,  $|H\rangle = c_{1\downarrow}^+ c_{3\downarrow}^+ c_{2\uparrow}^+ |0\rangle$ , and  $|I\rangle = c_{1\downarrow}^+ c_{2\downarrow}^+ c_{3\uparrow}^+ |0\rangle$ . For the spin-polarized system with  $S_z = -3/2$  there is only one possible configuration,  $|K\rangle = c_{1\downarrow}^+ c_{2\downarrow}^+ c_{3\downarrow}^+ |0\rangle$ .

The construction of the Hamiltonian matrix (9) in these bases of configurations requires the knowledge of Coulomb matrix elements. The Coulomb matrix elements in the itinerant basis are computed from Coulomb matrix elements in the localized basis as defined in Eq. (10), using the coefficients of the one-electron molecular eigenfunctions written in HO basis. The localized CMEs, Eq. (11), for the triple quantum dot potential of Fig. 1 consist of the onsite repulsion  $U = \langle rr|v|rr\rangle = 2.939179 Ry^*$ , interdot repulsion  $V = \langle rs|v|sr\rangle = 0.512857 Ry^*$ , and a number of small electron-electron scattering terms:  $\langle rr|v|rs\rangle = 0.004653 Ry^*$ ,  $\langle rs|v|st\rangle = 0.003446 Ry^*$ ,  $\langle rs|v|rs\rangle = 0.000049 Ry^*$ , and  $\langle rr|v|st\rangle = 0.000019 Ry^*$ . Upon rotation into the itinerant basis we find that the largest Coulomb matrix elements include direct repulsion on the lowest kinetic energy level  $\langle 11|v|11\rangle = 1.315811 Ry^*$  and on the degenerate excited state  $\langle 22|v|22\rangle = \langle 33|v|33\rangle = 1.730884 Ry^*$ . The direct and exchange interaction terms between the ground and excited states are  $\langle 12|v|21\rangle = 1.320137 Ry^*$  and  $\langle 12|v|12\rangle = 0.806983 Ry^*$ , respectively, while the scattering term  $\langle 11|v|22\rangle = 0.806983 Ry^*$ . Similar matrix elements are obtained for the degenerate shell of excited states:  $\langle 23|v|32\rangle = 0.918383 Ry^*$ ,  $\langle 23|v|23\rangle = 0.406251 Ry^*$ , and  $\langle 22|v|33\rangle = 0.406251 Ry^*$ . These Coulomb matrix elements are used in the construction of the three-electron Hamiltonian (9). After diagonalizing this Hamiltonian in the basis of configurations with  $S_z = -1/2$ :  $\{|i\rangle\} = \{|A\rangle, |B\rangle, |C\rangle, |D\rangle, |E\rangle, |F\rangle, |G\rangle, |H\rangle, |I\rangle\}$ , we obtain a spectrum of nine levels, shown in Fig. 5 (left). The nine eigenfunctions  $|i'\rangle$  are linear combinations of the basis configurations  $|i'\rangle = \sum_{i=A}^I A_i^{i'} |i\rangle$ . In the spectrum we can clearly distinguish two groups of levels separated by a large gap. The group in the upper part of the spectrum is composed of six energy levels and the group with lowest energy has three levels. We focus on this low-energy group. It is composed of a doubly degenerate

ground state and a non-degenerate first excited state, as shown in Fig. 4 (b), separated by the energy gap  $\Delta E = 0.0027 Ry^*$ . The doubly degenerate ground state has total spin  $S = 1/2$  and its two eigenfunctions  $|A'\rangle$  and  $|B'\rangle$  have their biggest contribution from the three electron configurations  $|A\rangle$  and  $|B\rangle$ , respectively. However, these states are highly correlated, with large contributions from other configurations. The eigenfunction  $|A'\rangle$ , with biggest contribution from the state  $|A\rangle$ , has also contributions from configurations  $|F\rangle, |H\rangle$  and  $|I\rangle$ :  $|A'\rangle = 0.6014|A\rangle + 0.5533|F\rangle - 0.4069|H\rangle - 0.4082|I\rangle$ , while the eigenfunction  $|B'\rangle$  with biggest contribution from state  $|B\rangle$ , has also contributions from states  $|C\rangle, |D\rangle$  and  $|E\rangle$ :  $|B'\rangle = 0.6014|B\rangle - 0.4075|C\rangle - 0.5533|D\rangle + 0.4075|E\rangle$ , as shown in Fig. 4 (c). The first excited state of this  $S_z = -1/2$  three-electron spectrum, state  $|GHI'\rangle$ , has total  $S = 3/2$ . Its eigenfunction  $|GHI'\rangle$  has approximately equal contribution from the three singly occupied molecular configurations:  $|G\rangle, |H\rangle$  and  $|I\rangle$ . Taking into account all four  $S_z$  subspaces, the ground state is four times degenerate (two levels with  $S_z = -1/2$  and two levels with  $S_z = 1/2$ ) and the first excited state is also four times degenerate (one level belonging to each  $S_z$  subspace).

In order to compare the microscopic model with the Hubbard model<sup>13</sup> we propose a modified LCHO-CI method. First, we carry out the  $s$ -LCHO one-electron calculations neglecting the overlap matrix. The resulting one-electron spectrum also shows a non-degenerate ground state and a doubly degenerate first excited state but with a bigger energy gap  $\Delta\epsilon_S^{Hub} = 3t = 0.201 Ry^*$ . Next, we apply the CI method to the  $S_z = -1/2$  subspace of Hamiltonian (9) but neglect all localized CME terms different than  $U$  and  $V$ . As in the itinerant electron basis, the three-electron spectrum obtained in this calculation shows two groups of levels, shown in the right-hand part of Fig. 5. The lower group conserves the structure of levels (a non-degenerate ground state and doubly-degenerate first excited state), although the energy gap is bigger  $\Delta E^{Hub} = 0.0111 Ry^*$ . On the other hand the upper group of levels not only shows bigger energy gaps, but the fifth and sixth excited states, nondegenerate in the full LCHO-CI calculation, become degenerate.

### C. Triple dot under bias

In this section we study the evolution of the energy spectrum of a three-electron molecule as a function of  $V_1$ , i.e., the depth of dot 1. The applied bias is kept smaller than the  $s$ - $p$

energy gap of one electron in one quantum dot in order to prevent population of the biased dot with two electrons. This is done so that we can attempt to map the three electron spectra onto the three spin spectra obtained in the Heisenberg model. We carry out our calculations for the case of  $s$ -HO orbitals as LCHO basis. Figure 6 (a) shows the resulting one-electron spectra as a function of bias of dot 1. The bias is measured in the units of the one-electron energy gap  $\Delta\epsilon_S = 0.095 Ry^*$ . When the dot is biased, the degenerate excited levels split due to the breaking of symmetry. This energy splitting increases with increasing bias. It is also observed that all energies decrease, but each of the three energies at a different rate. This can be understood by analyzing the evolution of orbitals associated with these energies. When the three dots are on resonance, the two excited levels are degenerate, and any linear combination of the two eigenfunctions  $|\xi_2\rangle$  and  $|\xi_3\rangle$ , defined in Eq. (15), is also an eigenfunction of the system corresponding to the same energy. This leads to equal probability of finding of the electron in each of the dots. However, if one of the dots is different, the excited level splits into two, and the wave functions  $|\xi_2\rangle$  and  $|\xi_3\rangle$  reflect this symmetry breaking. The first excited state  $|\xi_2\rangle$  has a contribution from the HO orbital corresponding to the first dot that decreases with increasing bias  $V_1$  (at the same time the contribution of this orbital increases in the ground state). On the other hand, the second excited state  $|\xi_3\rangle$  does not have any contribution from this orbital.

Figure 6(b) shows the spectra of three electrons with  $S_z = -1/2$  in the triple dot molecule for different values of  $V_1$ . We are interested in the three lowest levels as these are the ones relevant for quantum information processing and thus the ones that will be mapped onto Heisenberg spectra. Figure 7(a) shows the energies of these levels measured from the ground state energy. The degenerate ground state splits with bias. When bias is increased, the energy gap between the ground state and the first excited state increases, while the energy gap between the first and second excited states decreases.

#### D. Heisenberg model for three electrons

We now attempt to map the three-electron spectrum for the case in which dot 1 is biased onto the spectrum of the three-spin Heisenberg Hamiltonian (14) in the Jacobi basis. The mapping relies on the assumption that biasing dot 1 can be modeled by bias-dependent but equal parameters  $J_{12} = J_{13} = J$ , while  $J_{23}$  is different, but it may also be a function of

bias. With  $J_{12}$  equal  $J_{13}$ , the two Jacobi states  $|\beta_a\rangle$  and  $|\beta_b\rangle$  are eigenstates, with energies  $-\frac{3}{4}J_{av} - \frac{3}{4}(J_{23} - J_{av})$  and  $-\frac{3}{4}J_{av} + \frac{3}{4}(J_{23} - J_{av})$ , respectively, and  $|\beta_c\rangle$  is an eigenstate with energy  $+\frac{3}{4}J_{av}$ . The three eigenstates can be written in a way which emphasizes the role of the electron in the dot under bias (dot 1):  $|\beta_a\rangle = |\downarrow\rangle|S\rangle$  and  $|\beta_b\rangle = 1/\sqrt{3}|\downarrow\rangle|T_0\rangle - \sqrt{2/3}|\uparrow\rangle|T_-\rangle$ . Here the singlet and triplet states involving the second and third dot were written as  $|S\rangle = 1/\sqrt{2}(|\uparrow\downarrow\rangle - |\uparrow\downarrow\rangle)$ ,  $|T_0\rangle = 1/\sqrt{2}(|\downarrow\uparrow\rangle + |\uparrow\downarrow\rangle)$  and  $|T_-\rangle = |\downarrow\downarrow\rangle$ .

Figure 7(b) shows a plot of the energy spectrum of the Heisenberg Hamiltonian as a function of  $J/J_{23}$  from  $J = J_{23}$  to  $J = 0.93J_{23}$  with  $J > 0$  (antiferromagnetic ground state). By changing  $J$  from  $J_{23}$  to  $J = 0$  we drive the system from three equal dots to dot 1 totally decoupled. We compare this spectrum to that obtained in the full electronic calculation, shown in Fig. 7(a). As we can see, the two spectra behave in a similar manner as a function of bias of one of the dots ranging from three equal dots (zero bias) to a bias of  $\sim 1.5$  times the one-electron energy gap. We can now propose a procedure of finding the parameters  $J_{ij}$  by fitting the energy gaps in the Heisenberg spectrum,  $\Delta\varepsilon_{ab}^s = J_{23} - J$  and  $\Delta\varepsilon_{bc}^s = \frac{3}{2}J$ , to those in the LCHO-CI calculation. The value of  $J_{23}$  can be extracted at zero bias from the gap between the doubly-degenerate ground and the excited states. Assuming  $J_{23}$  to be independent of the bias of dot 1, two values of  $J$  - one from each gap of the spectrum - can be obtained and averaged for each step of bias. The numerical results show a decreasing value of the coupling constant  $J$  as the bias is being increased. This is the expected behavior because as we bias dot 1 the exchange of the electron in dot 1 with electrons in dots 2 and 3 decreases.

## V. CONCLUSIONS

We presented a computational LCHO-CI approach allowing for the simulation of exchange interactions in gated lateral quantum dot networks. The method was illustrated by analyzing the electronic properties of a lateral triple quantum dot network with one electron per dot. The LCHO-CI calculations show a low-energy spectrum composed of an antiferromagnetic ( $S = 1/2$ ) ground state separated by a small gap from the spin polarized ( $S = 3/2$ ) excited state, and separated by a large gap from the remaining excited levels involving double occupancy of quantum dots. We have shown that the behavior of these eight low-energy levels with bias of one quantum dot can be effectively reproduced by a Heisen-

berg spin model for a certain range of bias applied to quantum dots. For each value of bias, exchange coupling constants can be calculated from energy gaps in LCHO-CI model. We have thus established a connection between physical "external" parameters such as voltages, and exchange interaction among spins in the Heisenberg model.

## VI. ACKNOWLEDGMENT

We wish to thank A. Sachrajda, L. Gaudreau, A. Kam, and S. Studenikin for helpful discussions. The authors are grateful to the Canadian Institute for Advanced Research, and IPG to Spanish Ministerio de Educación y Ciencia grant No. AP-2004-0143 for financial support.

- 
- <sup>1</sup> M. A. Nielsen and I. L. Chuang, *Quantum Computation and Quantum Information* (Cambridge University Press, 2000).
  - <sup>2</sup> J. A. Brum and P. Hawrylak, *Superlattices Microstruct.* **22**, 431 (1997).
  - <sup>3</sup> D. Loss and D. P. DiVincenzo, *Phys. Rev. A* **57**, 120 (1998).
  - <sup>4</sup> D. P. DiVincenzo, D. Bacon, J. Kempe, G. Burkard, and K. B. Whaley, *Nature* **408**, 339 (2000).
  - <sup>5</sup> M. Ciorga, A. S. Sachrajda, P. Hawrylak, C. Gould, P. Zawadzki, S. Jullian, Y. Feng, and Z. Wasilewski, *Phys. Rev. B* **61**, 16315 (2000).
  - <sup>6</sup> S. Tarucha, D. G. Austing, T. Honda, R. J. van der Haage, and L. P. Kouwenhoven, *Phys. Rev. Lett.* **77**, 3613 (1996).
  - <sup>7</sup> A. W. Holleitner, R. H. Blick, A. K. Hüttel, K. Eberl, and J. P. Kotthaus, *Science* **297**, 70 (2002).
  - <sup>8</sup> M. Pioro-Ladriere, R. Abolfath, P. Zawadzki, J. Lapointe, S. Studenikin, A. S. Sachrajda, and P. Hawrylak, *Phys. Rev. B* **72**, 125307 (2005).
  - <sup>9</sup> F. H. Koppens, J. A. Folk, J. M. Elzerman, R. Hanson, L. H. W. van Beveren, I. T. Vink, H. P. Tranitz, W. Wegscheider, L. P. Kouwenhoven, and L. M. K. Vandersypen, *Science* **309**, 1346 (2005).
  - <sup>10</sup> J. R. Petta, A. C. Johnson, J. M. Taylor, E. A. Laird, A. Yacoby, M. D. Lukin, C. M. Marcus, M. P. Hanson, and A. C. Gossard, *Science* **309**, 2180 (2005).

- <sup>11</sup> T. Hatano, M. Stopa, and S. Tarucha, *Science* **309**, 268 (2005).
- <sup>12</sup> L. Gaudreau, S. Studenikin, A. Sachrajda, P. Zawadzki, A. Kam, J. Lapointe, M. Korkusinski, and P. Hawrylak, *Phys. Rev. Lett.* **97**, 036807 (2006).
- <sup>13</sup> M. Korkusinski, I. Puerto Gimenez, P. Hawrylak, L. Gaudreau, S. A. Studenikin, and A. S. Sachrajda, *Phys. Rev. B* **75**, 115301 (2007).
- <sup>14</sup> A. Mizel and D. A. Lidar, *Phys. Rev. Lett* **92**, 077903 (2004).
- <sup>15</sup> A. Mizel and D. A. Lidar, *Phys. Rev. B* **70**, 115310 (2004).
- <sup>16</sup> R. Woodworth, A. Mizel, and D. A. Lidar, *J. Phys.: Condens. Matter* **18**, S721 (2006).
- <sup>17</sup> P. Hawrylak and M. Korkusinski, *Solid State Commun.* **136**, 508 (2005).
- <sup>18</sup> Y. S. Weinstein, S. C. Hellberg, and J. Levy, *Phys. Rev. A* **72**, 020304 (2005).
- <sup>19</sup> V. W. Scarola, K. Park, and S. Das Sarma, *Phys. Rev. Lett.* **93**, 120503 (2004).
- <sup>20</sup> J. Kyriakidis, M. Pioro-Ladriere, M. Ciorga, A. S. Sachrajda, and P. Hawrylak, *Phys. Rev. B* **66**, 035320 (2002).
- <sup>21</sup> V. W. Scarola and S. D. Sarma, *Phys. Rev. A* **71**, 032340 (2005).



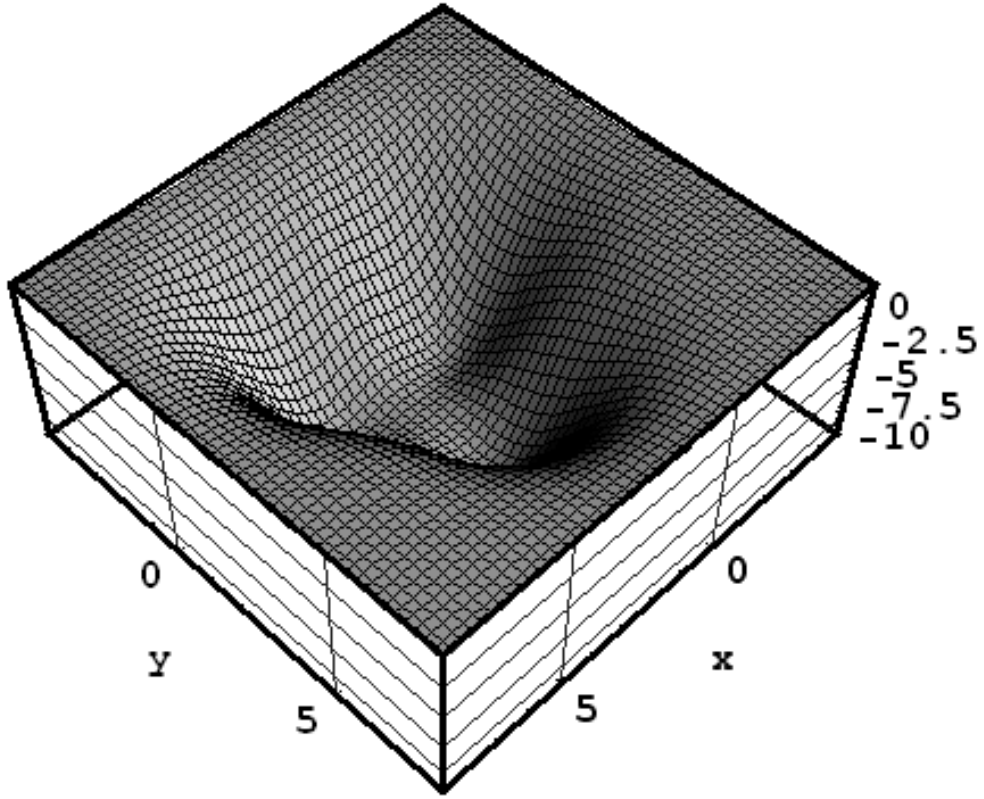


FIG. 1: 3D plot of the triple quantum dot potential with equal dots characterized by depths  $V_i = 10 Ry^*$  and widths  $d_i = 2.3 a_B^*$ . The dots are centered at  $(0,0)$ ,  $(4,0)$  and  $(2,3.4641)$  forming an equilateral triangle with side lengths  $4 a_B^*$ .

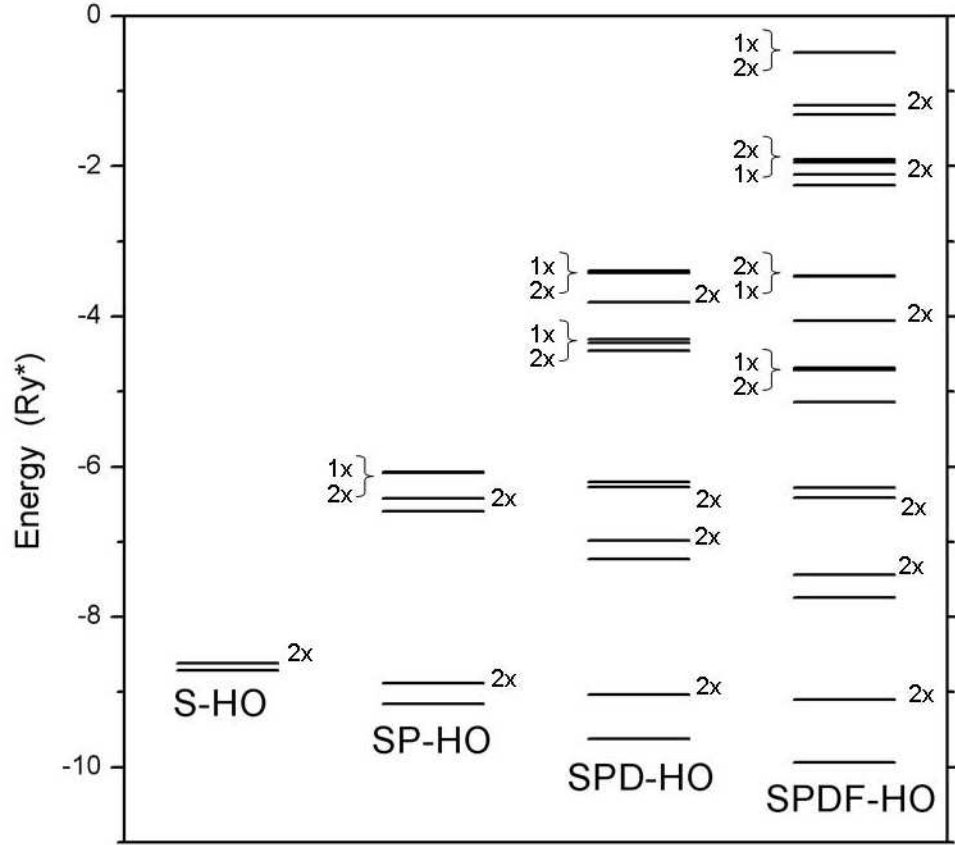


FIG. 2: Energy levels of one electron in the triple quantum dot potential of Fig. 1 calculated with the LCHO method as a function of the number of HO basis states .

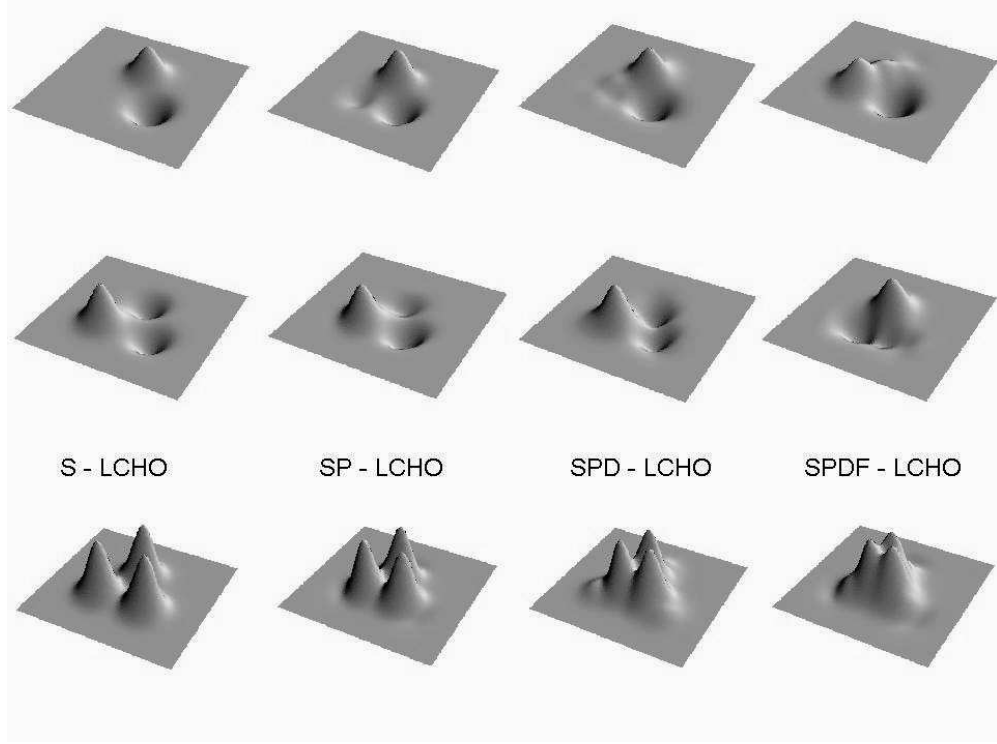


FIG. 3: Comparison of the three lowest energy eigenfunctions ( $|\xi_1\rangle$ ,  $|\xi_2\rangle$  and  $|\xi_3\rangle$ ) of one electron in a triple quantum dot, calculated with the LCHO method using different numbers of HO wave functions as basis. Eigenfunctions at the bottom correspond to the ground state,  $|\xi_1\rangle$ , and the two at the top,  $|\xi_2\rangle$  and  $|\xi_3\rangle$ , correspond to the degenerate excited states.

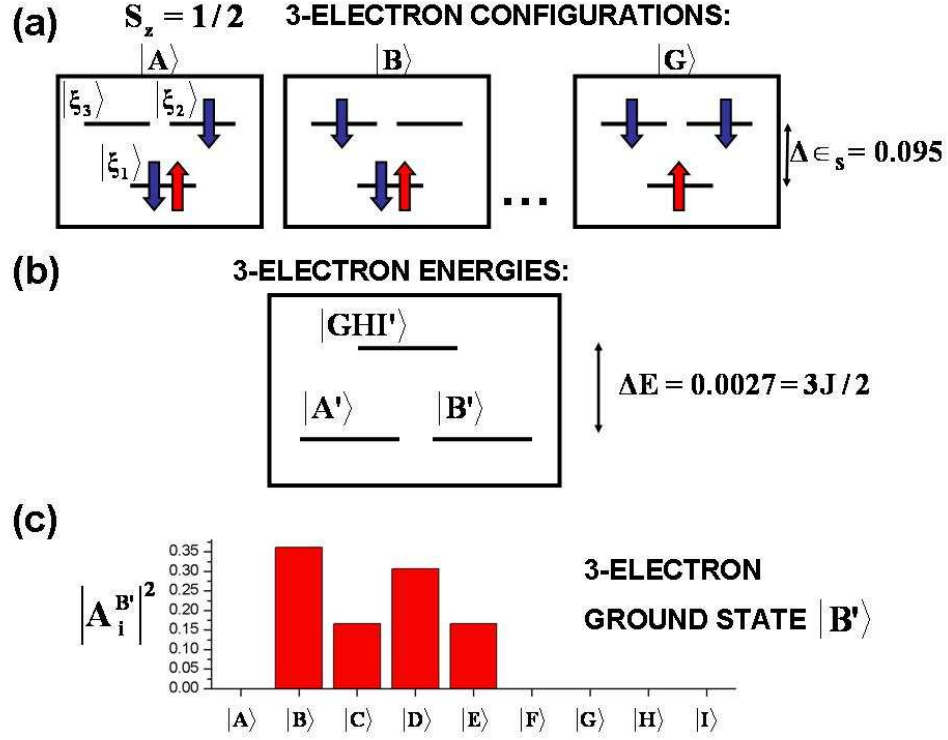


FIG. 4: (a) Examples of three-electron configurations that form the basis for CI calculations. (b) The lowest group of levels of the three electron spectrum. (c) Contribution of different configurations to one of the two states of the ground level.

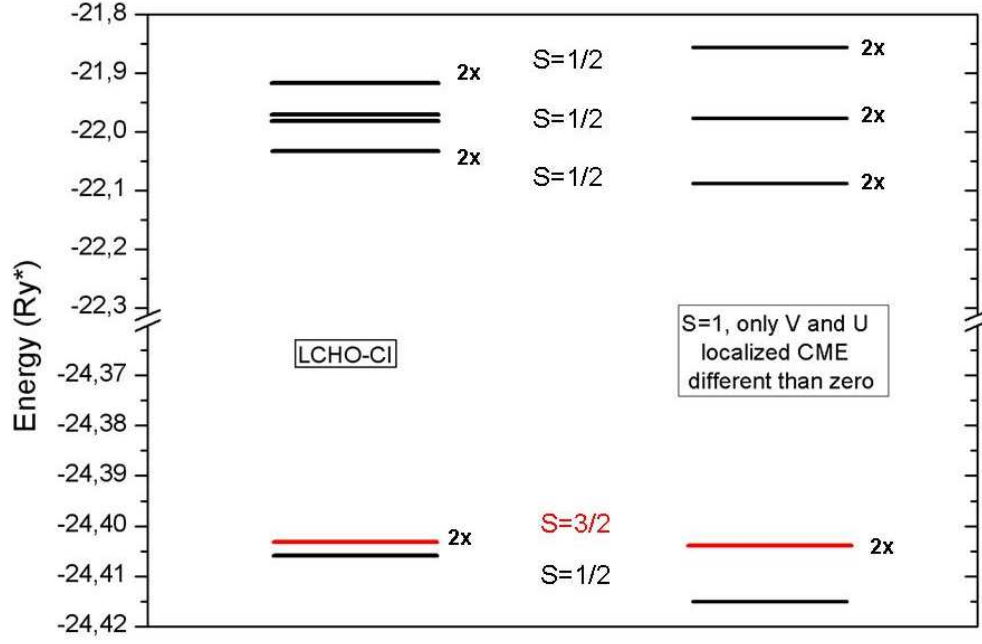


FIG. 5: Left: spectrum of three electrons with  $S_z = -1/2$  in the triple quantum dot calculated with LCHO-CI method. Right: spectrum of three electrons with  $S_z = -1/2$  in the triple dot calculated with LCHO-CI method but neglecting the overlap matrix and all CMEs except for  $U = \langle rr|v|rr \rangle$  and  $V = \langle rs|v|sr \rangle$ .

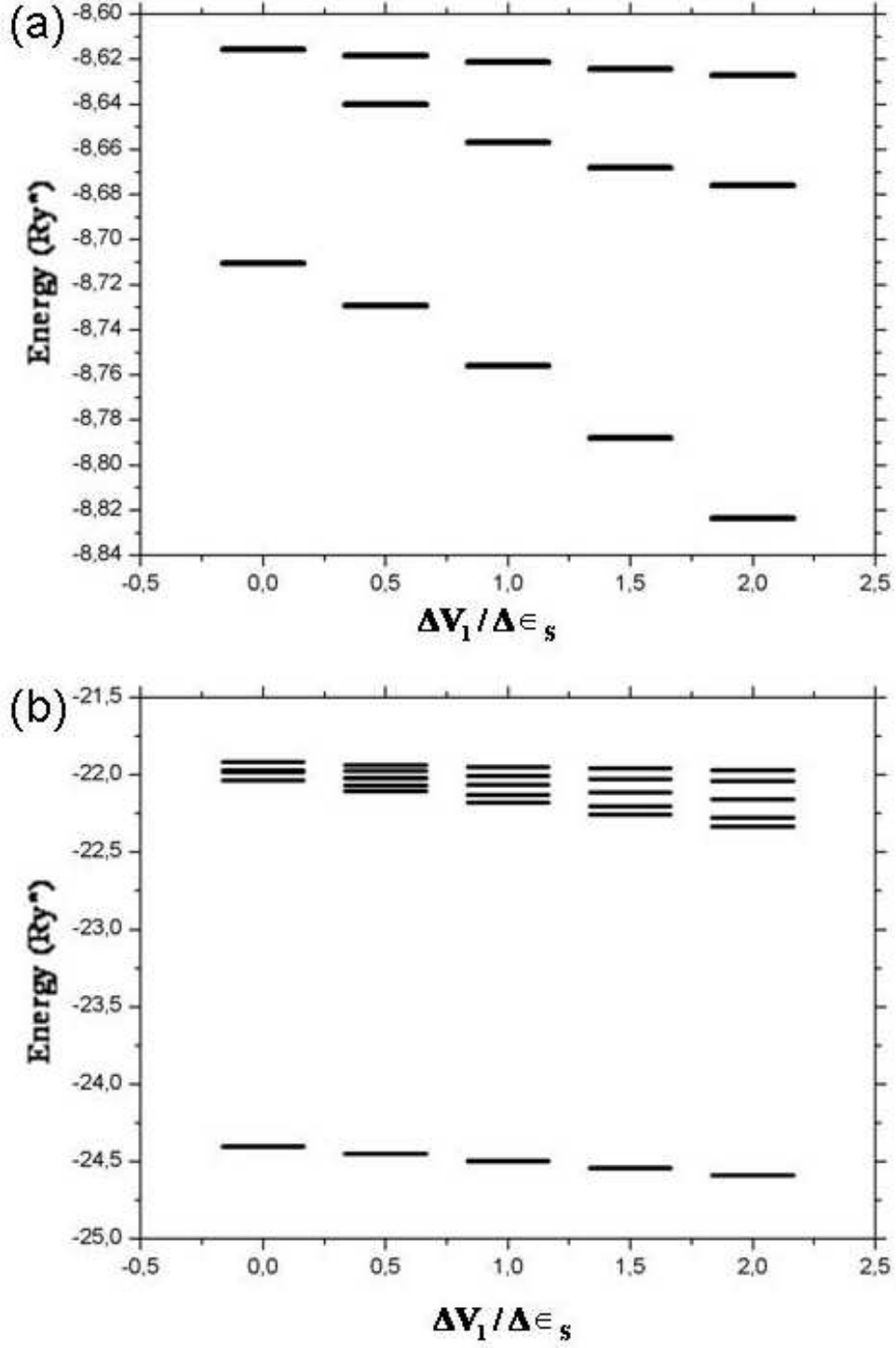


FIG. 6: (a) Spectra of one electron in the triple dot as a function of bias of dot 1. (b) Spectra of three electrons with  $S_z = -1/2$  in the triple dot as a function of bias of dot 1, calculated with the LCHO-CI method considering  $s$ -HO levels in the LCHO calculation.

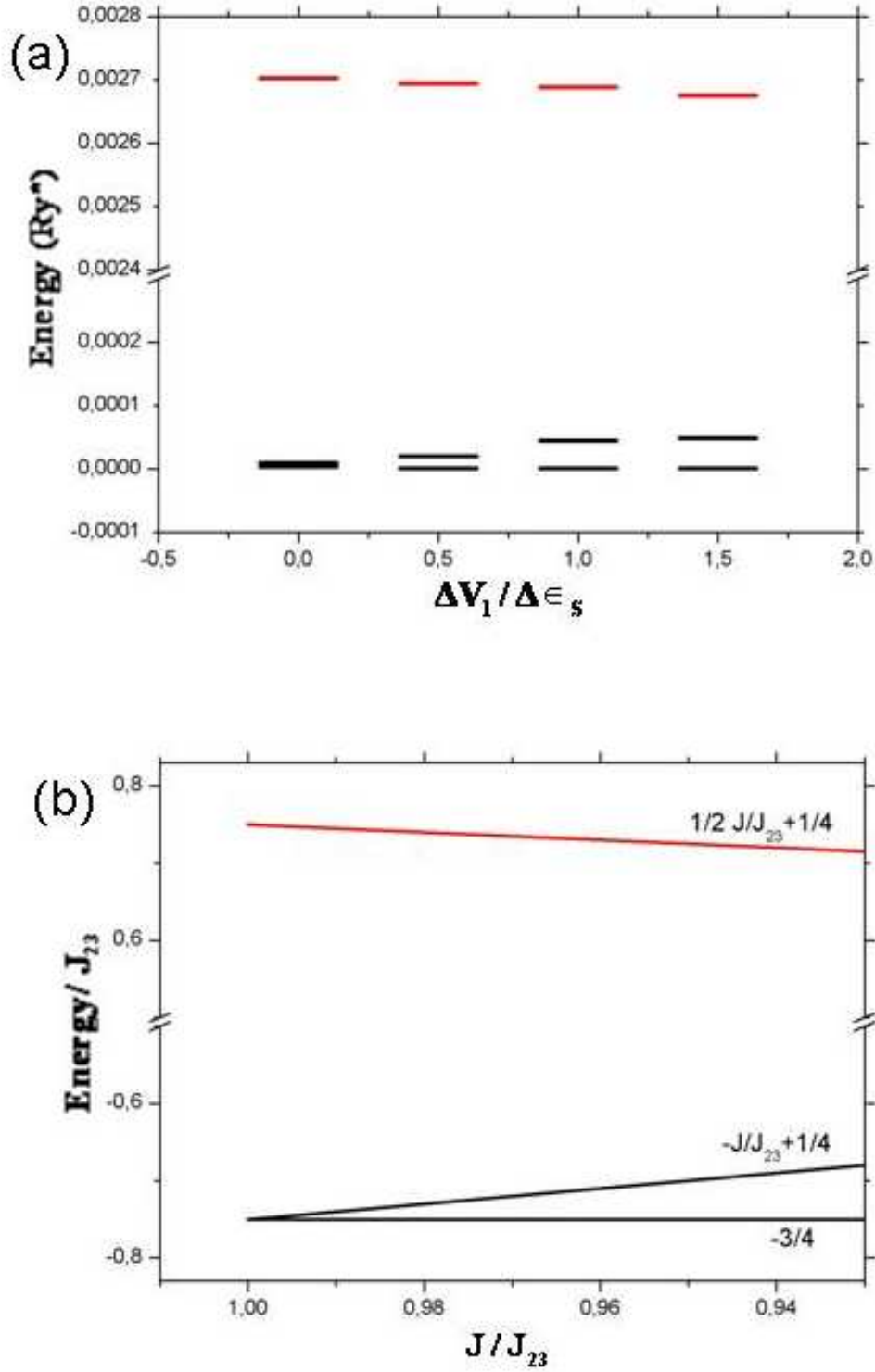


FIG. 7: (a) Three lowest levels of spectra of three electrons in the triple dot (Fig. 6), with the ground state energy as a reference level, as a function of bias of dot 1. (b) Spectra of three electrons  $S_z = -1/2$  given by Heisenberg model with  $J_{12} = J_{13} \equiv J$  plotted as a function of  $J/J_{23}$  with  $J$  varying from  $J_{23}$  to  $0.93J_{23}$ .